BASE-ISOLATED BUILDING CONNECTED TO ADJACENT BUILDING USING VISCOUS DAMPERS

Vasant A. Matsagar[1] and R.S. Jangid[2]

ABSTRACT

Seismic response of multi-storied base-isolated building on various isolation systems connected using viscous dampers to an adjacent dissimilar base-isolated or fixed-base building is investigated. The multi-storied buildings are modeled as a shear type structures with lateral degree-of-freedom at each floor, which are connected at different floor levels by the viscous dampers. Performance of this novel combination is studied by deriving the governing equations of motion and solving it in the incremental form using Newmark's step-by-step method of integration. The variation of top floor absolute acceleration and bearing displacement under different real earthquake ground motions is computed to study the behavior and effectiveness of the connected systems. It is concluded that connecting the two adjacent base-isolated buildings with the viscous dampers is helpful in controlling large bearing displacement in the base-isolated structures; thereby, eliminating isolator damages arising due to instability at large displacement or pounding with adjacent structures during the earthquakes. Parametric studies are also performed to identify optimal parameters such as damper damping and distribution pattern of viscous dampers to achieve the maximum response reduction in the damper-linked adjacent buildings. The connection of viscous dampers to adjacent structures are found to be most effective when: (i) the adjacent base-isolated and fixed-base buildings are connected, (ii) dissimilar isolation systems are used for the two adjacent buildings, (iii) the time periods of adjacent structures are well separated, and (iv) the superstructure flexibility is higher.

Keywords: adjacent building, base isolation, bearing displacement, earthquake, elastomeric bearing, pounding, sliding system, superstructure acceleration, viscous damper.

1.0 INTRODUCTION

Base isolation technique has emerged as a viable alternative in seismic prone areas to reduce the vulnerability of structural systems subjected to earthquakes. The base isolation increases lateral flexibility of the entire base-isolated structure and increases its effective damping through the energy dissipated in the isolation system. The dynamic response of a base-isolated structure, therefore, is considerably reduced when compared to its counterpart, the fixed-base structure, as documented in sizeable literature available on the base isolation [1-3]. In seismic isolation, the fundamental frequency is decreased and kept away from the predominant frequency range of most of the earthquake ground motions. Although, with the decreasing frequency, floor accelerations are reduced helping to limit the damage to the structure, the increased displacement at isolation level calls upon necessity of maintaining adequate separation gap

[1] *Graduate Student, Department of Civil Engineering, Indian Institute of Technology Bombay, Powai, Mumbai - 400 076 (India).*

[2] *Associate Professor, Department of Civil Engineering, Indian Institute of Technology Bombay (e-mail: rsjangid@civil.iitb.ac.in)*

distance to incorporate the large bearing displacement. Consequently, the separation gap requirement in case of base-isolated structure is more than the fixed-base structure.

In modern cities, however, due to high value of land space, limited availability of land and preference for centralized services, there is a tendency to construct the buildings in close proximity to each other without maintaining proper separation gap distances. During a possible earthquake event, these buildings vibrate vigorously and may become a cause for sever damage because of mutual pounding. The 1985 Mexico City and 1989 Loma Prieta earthquakes are the typical examples of the large-scale damage caused by the structural pounding. In view of this, the latest building codes have made requirements for base-isolated structures more stringent [4] specifying accommodation of larger bearing displacements during the Maximum Capable Earthquakes (MCE) and has suggested need for supplemental damping devices. In overcoming this dilemma, present study in this paper suggests the use of viscous damper connections between the adjacent structures.

The papers reported by Housner *et al.* [5] and Soong and Spencer [6] provide detailed review of earlier and recent studies made on structural control and supplemental energy dissipation devices and its applications to seismic protection of the buildings. To avoid pounding damages during earthquakes, the concept of linking adjacent fixed-base buildings is introduced and verified analytically and experimentally by number of researchers [7-14]. These papers also delineate the practical feasibility of the proposed scheme of connecting the adjacent buildings using dampers. However, authors have not come across studies with regard to mitigation of pounding and/ or impact damages in case of base-isolated adjacent structures achieved through incorporation of damper linkages between the two. Therefore, it would be interesting to investigate the effectiveness of connecting the base-isolated building with the adjacent building, as an alternative for protection against possible destruction due to pounding because of inadequate separation gap distance provided between the two and improving seismic performance of the existing fixed-base buildings.

This paper investigates the advantages of connecting base-isolated building to the adjacent base-isolated or fixed-base building using viscous dampers. The main objectives of this study are to investigate: (i) the dynamic characteristics of base-isolated building connected to the adjacent base-isolated or fixed-base building using discrete linear viscous dampers; (ii) the optimum parameters for damper damping and location to achieve maximum response reduction; and (iii) the effectiveness of such connections under different earthquakes and properties of the adjacent buildings such as isolation time period and superstructure flexibility.

2.0 MODELING OF ADJACENT STRUCTURES

Figure 1 shows two structural models under consideration depicting multi-degree-of-freedom shear models with rigid floors. Figure 1(a) shows l-storey base-isolated building connected through viscous dampers at different floors to an adjacent m-storey base-isolated building. In Figure 1(b), similar viscous damper connected system with l-storey base-isolated building mounted on various isolation systems connected to an adjacent m-storey fixed-base building is shown. The masses in these models are assumed to be lumped at each floor level and the stiffness is provided by axially inextensible mass-less columns. Both the adjacent connected buildings are assumed to behave linearly elastic and receive same earthquake ground motion in horizontal direction. The soil-structure interaction effects are not taken into consideration. For both the buildings, the mass at all the floor levels is kept constant while the stiffness is varied to achieve the desired fundamental time periods as fixed-base condition.

These adjacent buildings are connected at different floor levels by the linear viscous dampers to serve as energy dissipation mechanism. A typical viscous damper consists of viscous material in the form of either liquid (silicon oil) or solid (special rubbers or acrylics), dissipating the energy (i) by the principle of flow through orifice and (ii) through deformation of viscous fluid or special solid material. Fluid viscous damper [15] consists of a stainless steel piston head with number of small bronze orifices, a piston rod, casing filled with viscous fluid and high strength seals at end caps. Such viscous dampers are represented using a phenomenological model of a dashpot.

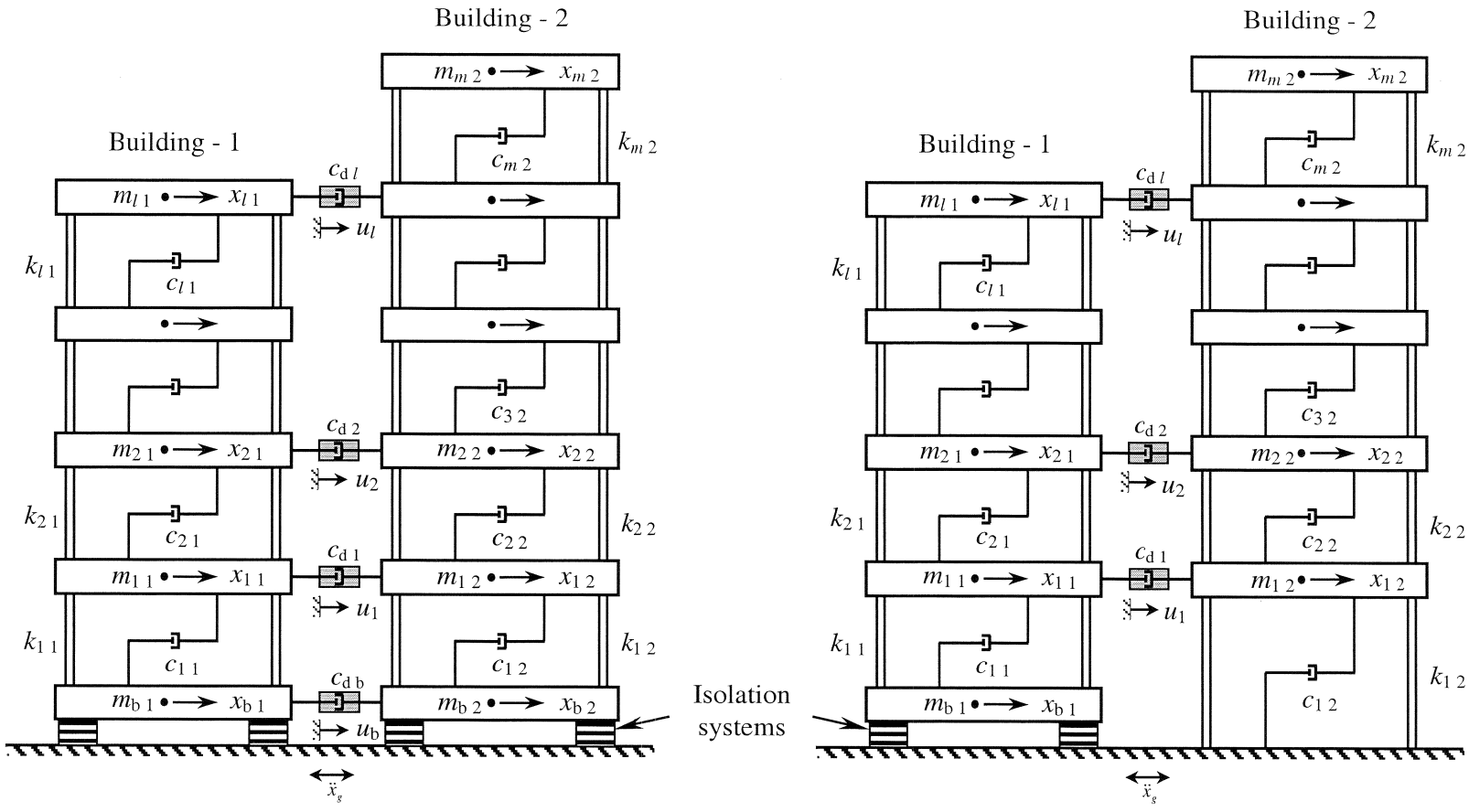

(a) Two base-isolated buildings

(b) Base-isolated and fixed-base buildings

Figure 1. Mathematical model of viscous dampers connected to adjacent buildings.

3.0 GOVERNING EQUATIONS OF MOTION

For the systems under consideration, the governing equations of motion are obtained by considering equilibrium of forces at the location of each degree-of-freedom during seismic excitations. When these adjacent buildings are not connected with the damper links, they act independently having the dynamic degrees-of-freedom of l and m, at each floor of Buildings 1 and 2, respectively. Two individual sets of governing equations of motion for such systems under earthquake excitation can be expressed in the following form

$$[M]\{\ddot{x}\}+[C]\{\dot{x}\}+[K]\{x\}+[D]\{F_b\}=-[M]\{r\}(\ddot{x}_g) \quad (1)$$

where $[M]$, $[C]$ and $[K]$ are the mass, damping and stiffness matrices, respectively; $\{x\}$, $\{\dot{x}\}$, $\{\ddot{x}\}$ are unknown floor displacement, velocity and acceleration vectors, respectively; $\{F_b\}$ is restoring force vector in the isolation system; $[D]$ is location matrix for the isolator forces; $\{r\}$ is vector of influence coefficients; and $\ddot{x}_g$ is earthquake ground acceleration.

Owing to the introduction of viscous dampers as connecting links for the two adjacent buildings, it converts to a connected system with $(l+m)$ lateral degrees-of-freedom. The governing equation of motion for such a connected system is of similar form as in Equation (1) in which, $\{x\}=\{x_{11}, x_{21}, \ldots x_{l1}, x_{12}, x_{22}, \ldots x_{m2}\}^T$ is the unknown floor displacement vector. Here, the second subscripts, i = 1 and 2 denote the quantities pertaining to the connected Buildings 1 and 2, respectively. The mass, damping and stiffness matrices are suitably formulated for the connected system. Similarly, the governing equation of motion for the fixed-base building can be obtained from Equation (1), during unconnected and connected cases. The isolation restoring forces $\{F_b\}$, in Equation (1), for the three different types of isolation systems used in the present study namely, laminated rubber bearings, lead-rubber bearings and friction pendulum systems placed under the base-isolated buildings are derived as follows.

3.1 Laminated Rubber Bearing

The laminated rubber bearing (LRB) represents the commonly used elastomeric bearings. The basic components of LRB are steel and rubber plates built in alternate layers [16]. The dominant feature of LRB is parallel action of linear spring and damping as shown schematically in Figure 2(a).

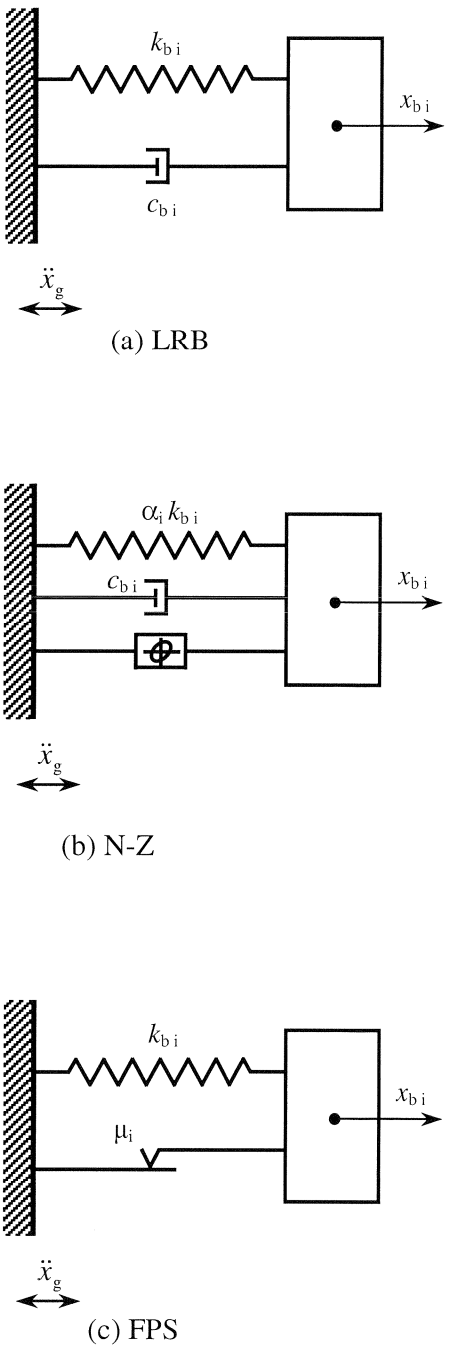

Figure 2. Schematic models of isolation systems.

The LRB exhibits high-damping capacity, horizontal flexibility and high vertical stiffness. The damping constant of the system varies considerably with strain level of the bearing (generally of the order of 10 percent). The system operates by decoupling the structure from horizontal components of earthquake ground motion by interposing a layer of low horizontal stiffness between the structure and its foundation. The isolation effects in this type of system are produced not by absorbing the earthquake energy but by deflecting through the dynamics of the system. Usually, there is a large difference in damping of the structure and the isolation device, which makes the system non-classically damped. The restoring force, F_b developed in the LRB is given by

$$F_{bi} = c_{bi}\dot{x}_{bi} + k_{bi}x_{bi} \qquad (i = 1, 2) \tag{2}$$

where c_{bi} and k_{bi} are damping and stiffness of LRB, respectively.

The stiffness and damping of the LRB are selected such that to provide the specific values of two parameters characterizing the system namely, isolation time period (T_{bi}) and damping ratio (ξ_{bi}), defined as

$$T_{bi} = 2\pi\sqrt{\frac{M_i}{k_{bi}}} \qquad (i = 1, 2) \tag{3}$$

$$\xi_{bi} = \frac{c_{bi}}{2 M_i \omega_{bi}} \qquad (i = 1, 2) \tag{4}$$

where $M_i = \left(m_{bi} + \sum_{j=1}^{l \text{ or } m} m_{ji} \right)$ is the total mass of the base-isolated building; m_{bi} is the mass of the base-raft of i^{th} building; m_{ji} is the mass of j^{th} floor of i^{th} building; $\omega_{bi} = 2\pi / T_{bi}$ is the isolation frequency.

3.2 Lead-Rubber Bearing

The second category of elastomeric bearings is lead-rubber bearings [17] as shown schematically in Figure 2(b). This system provides the combined features of vertical load support, horizontal flexibility, restoring force and damping in a single unit. These bearings are similar to the LRB but a central lead core is used to provide an additional means of energy dissipation. These bearings are widely used in New Zealand and referred as N-Z systems. The energy absorbing capacity by the lead core reduces the lateral displacements of the isolator. The force-deformation behavior of the N-Z system is generally represented by non-linear characteristics following a hysteretic nature. For the present study, Wen's model [18] is used to characterize the hysteretic behavior of the N-Z systems. The restoring force developed in these isolation systems is given by

$$F_{bi} = c_{bi}\dot{x}_{bi} + \alpha_i k_{bi} x_{bi} + (1-\alpha_i) F_{yi} Z_i \qquad (i = 1, 2) \tag{5}$$

where F_{yi} is yield strength of the bearing; α_i is an index which represent the ratio of post to pre-yielding stiffness; k_{bi} is initial stiffness of the bearing; c_{bi} is viscous damping of the bearing; and Z_i is a non-dimensional hysteretic displacement component satisfying the following non-linear first order differential equation expressed as

$$q_i \frac{dZ_i}{dt} = A\dot{x}_{bi} + \beta \left| \dot{x}_{bi} \right| Z_i \left| Z_i \right|^{n-1} - \tau \dot{x}_{bi} \left| Z_i \right|^n \qquad (i = 1, 2) \tag{6}$$

where q_i is isolator yield displacement; the dimensionless parameters A, β, τ and n are selected such that predicted response from the model closely matches with the experimentally obtained results. The parameter n is an integer constant, which controls smoothness of the transition from elastic to inelastic response.

The N-Z system is characterized by isolation period (T_{bi}), damping ratio (ξ_{bi}) and normalized yield strength, Q_i i.e. $Q_i = F_{yi} / W_i$ (where $W_i = M_i g$ is the total weight of the building; and g is acceleration due to the gravity). The bearing parameters, T_{bi} and ξ_{bi} are computed from the Equations (3) and (4), respectively using the post-yield stiffness of the bearing. The other parameters of the N-Z system are held constant with q_i = 2.5 cm, A = 1, $\beta = \tau = 0.5$ and n = 2.

3.3 Friction Pendulum System

One of the most popular and effective techniques for seismic isolation is through the use of sliding isolation devices. The sliding systems exhibit excellent performance under a variety of severe earthquake loading and are very effective in reducing large levels of the superstructure acceleration. These isolators are characterized by insensitivity to the frequency content of earthquake excitation, because of the tendency of sliding system to reduce and spread the earthquake energy over a wide range of frequencies. Another advantage of sliding isolation systems over the conventional rubber bearings is that, because of development of the frictional force at the base, it is proportional to the mass of the structure and the centre of mass and centre of resistance of the sliding support coincides. Consequently, the torsional effects produced by an asymmetric building are diminished. The concept of sliding bearings is combined with the concept of a pendulum type response, resulting to a conceptually interesting seismic isolation system known as a friction pendulum system (FPS) [19] as shown schematically in Figure 2(c). In FPS, the isolation is achieved by means of an articulated slider on spherical, concave chrome surface. The slider is faced with a bearing material which when in contact with the polished chrome surface results in development of the friction force while concave surface produces restoring force. The resisting force provided by the FPS is

$$F_{bi} = k_{bi} x_{bi} + F_{xi} \qquad (i = 1, 2) \tag{7}$$

where k_{bi} is bearing stiffness provided by virtue of inward gravity action at the concave surface; and F_{xi} is the frictional force.

The system is characterized by isolation time period (T_{bi}) that depends upon radius of curvature of concave surface; and friction coefficient (μ_i). The isolation stiffness, k_{bi} is adjusted such that the specified value of the isolation time period evaluated by the Equation (3) is achieved.

3.4 Viscous Damper

The damping force generated in the viscous damper, which is essentially proportional to the relative velocity of the piston head with respect to the damper casing, is expressed as

$$\{F_d\} = [C_d]\{\dot{u}_b, \dot{u}_1, \dot{u}_2, ..., \dot{u}_l\}^T \tag{8}$$

where $\{\dot{u}_b, \dot{u}_1, \dot{u}_2, ..., \dot{u}_l\}$ and $\{u_b, u_1, u_2, ..., u_l\} = \{x_{b1}, x_{11}, x_{21}, ..., x_{l1}\} - \{x_{b2}, x_{12}, x_{22}, ..., x_{l2}\}$ are vectors of relative velocity and displacement between the damper connected floors of the adjacent buildings and over-dot denotes the derivative with respect to time. The damper damping matrix for the array of dampers placed along height of the adjacent structures, is expressed as

$$[C_d] = \text{diag}[c_{db}, c_{d1}, c_{d2}, ..., c_{dl}] \tag{9}$$

where $c_{db}, c_{d1}, c_{d2}, ..., c_{dl}$ are the damper damping coefficients at different floor levels. The total external damping added in the form of connection links between the two adjacent buildings is expressed as a non-dimensional parameter

$$\eta_d = \frac{c_{db} + \sum c_{dj}}{2\xi_e \omega_e \sum M_i} \qquad (i = 1, 2 \text{ and } j = 1, l) \tag{10}$$

where ξ_e is equivalent viscous damping ratio taken as 10 percent; and ω_e is equivalent isolation frequency considered as π rad/sec. This implies that the total damper damping is expressed in proportion with properties of an equivalent LRB having damping ratio of 10 percent and isolation time period of 2 sec.

4.0 SOLUTION OF EQUATIONS OF MOTION

Classical modal superposition technique cannot be employed to obtain solution of equations of motion because the system is non-classically damped due to difference in damping in the isolation system as compared to the damping in superstructure of the base-isolated building as well as the damper-links. Therefore, for different earthquakes, the equations of motion are solved numerically using Newmark's method of step-by-step integration; adopting linear variation of acceleration over a small time interval of Δt. The time interval for solving the equations of motion is taken as 0.02/20 sec (i.e. Δt = 0.001 sec). At each time instant, the responses namely, the accelerations, base shear and displacements are obtained at each floor level of the two adjacent buildings.

5.0 NUMERICAL STUDY

Seismic response of two dissimilar adjacent multi-storied buildings, connected using viscous dampers, either both or one of them supported on isolation devices is investigated here. The multi-degree-of-freedom shear models of the adjacent buildings are used, with linear viscous damping devices at different floor levels as connecting links. The earthquake motions selected for the parametric study are: (i) N00E component of 1989 Loma Prieta earthquake (18th October 1989) recorded at Los Gatos Presentation Centre; (ii) N90S component of 1994 Northridge earthquake (17th January 1994) recorded at Sylmar Converter station; and (iii) N00S component of 1995 Kobe earthquake (17th January 1995) recorded at JMA. The peak ground acceleration (PGA) of Loma Prieta, Northridge and Kobe earthquake motions are 0.56g, 0.59g and 0.82g, respectively.

5.1 Damper Connected Two Adjacent Base-isolated Buildings

The time histories of top floor acceleration, bearing displacement and damper displacement for 3 and 5 -storied adjacent base-isolated buildings using LRB ($T_{b1} = 2\,\text{sec}$ and $\xi_{b1} = 0.1$) and N-Z ($T_{b2} = 3\,\text{sec}$, $\xi_{b2} = 0.05$, $q_2 = 25\,\text{mm}$ and $Q_2 = 0.05$) system, respectively under the Loma Prieta, 1989 earthquake for unconnected and connected cases are plotted in Figure 3. The associated response with the fixed-base response of the buildings is also shown for the purpose of comparison. The total external normalized damping value of $\eta_d = 2$ is chosen with damper connections provided at all the floors having equal values of damping coefficients. The η_d equal to 2 indicates that damper damping is twice of that provided by the LRB isolator; and damper damping can be chosen appropriately by conducting parametric studies, as described later in the paper to obtain maximum response reduction. It is observed that the bearing displacement in the base-isolated Building 2, (x_{b2}) has decreased when connected to the adjacent base-isolated Building 1 using viscous dampers, while the bearing displacement in the base-isolated Building 1, (x_{b1}) has increased marginally. The top floor acceleration in isolated Building 1, ($\ddot{x}_{t1}$) with LRB and Building 2, ($\ddot{x}_{m2}$) with N-Z system are decreased substantially when these two buildings are connected together (Refer also to the peak response shown in Table 1 later, for more clarity). The top floor acceleration of 0.550g and 0.380g reduces to 0.398g and 0.366g, respectively for the base-isolated Buildings 1 and 2, respectively. It is concluded from the above observations that connecting the adjacent base-isolated buildings with viscous dampers lead to reduction in the bearing displacement and superstructure acceleration for soft building while the stiffer building experiences either decrease or marginal increase in its response during earthquake motion. However, the greatest advantage of such links introduced here is that, the impact between adjacent floors is avoided by virtue of dampers so that the consequences of pounding failures are altogether eliminated even during vigorous shaking at the time of occurrence of earthquakes. In addition, these links also avoid the damage of isolators due to possible impacts on the adjoining ground structures. Figure 3 also shows the plot of the displacement across the connecting viscous dampers. It is seen that the maximum differential floor displacement across the damper is 199.8 mm under the Loma Prieta, 1989 excitation for the damper connected system in consideration.

Table 1 shows the peak response of unconnected and connected adjacent base-isolated buildings for the total normalized external damping, $\eta_d = 2$. For the purpose of demonstration, a 3-storied Building 1 mounted on LRB, is considered adjacent to the other 5-storied Building 2 isolated using N-Z system, with the isolation parameters same as mentioned earlier. Performance of these two buildings is observed during the cases such as (a) fixed-base, (b) isolated unconnected and (c) isolated connected at all floors using viscous dampers with equal distribution of total external damping amongst all the dampers. When viscous damper links are introduced, the bearing displacement in both the base-isolated Buildings 1 and 2 decreases compared to the unconnected cases under Loma Prieta, 1989, Northridge, 1994 and Kobe, 1995 earthquakes. The effect of damper linkages is found more on the bearing displacement as compared to that on the top floor acceleration. The top floor acceleration in base-isolated Building 1 decreases largely; while in few cases the top floor acceleration in Building 2 may increase marginally for selected external damping. For

this reason, it is to be noted that the selection of proper values of damper damping coefficients and distribution along the height of the connected system is highly essential to obtain the maximum response reduction. Similar trend of decrease in bearing displacement and top floor acceleration is observed when FPS ($T_{b2} = 3\,\text{sec}$ and $\mu_2 = 0.05$) used as isolation system for Building 2 connected using viscous

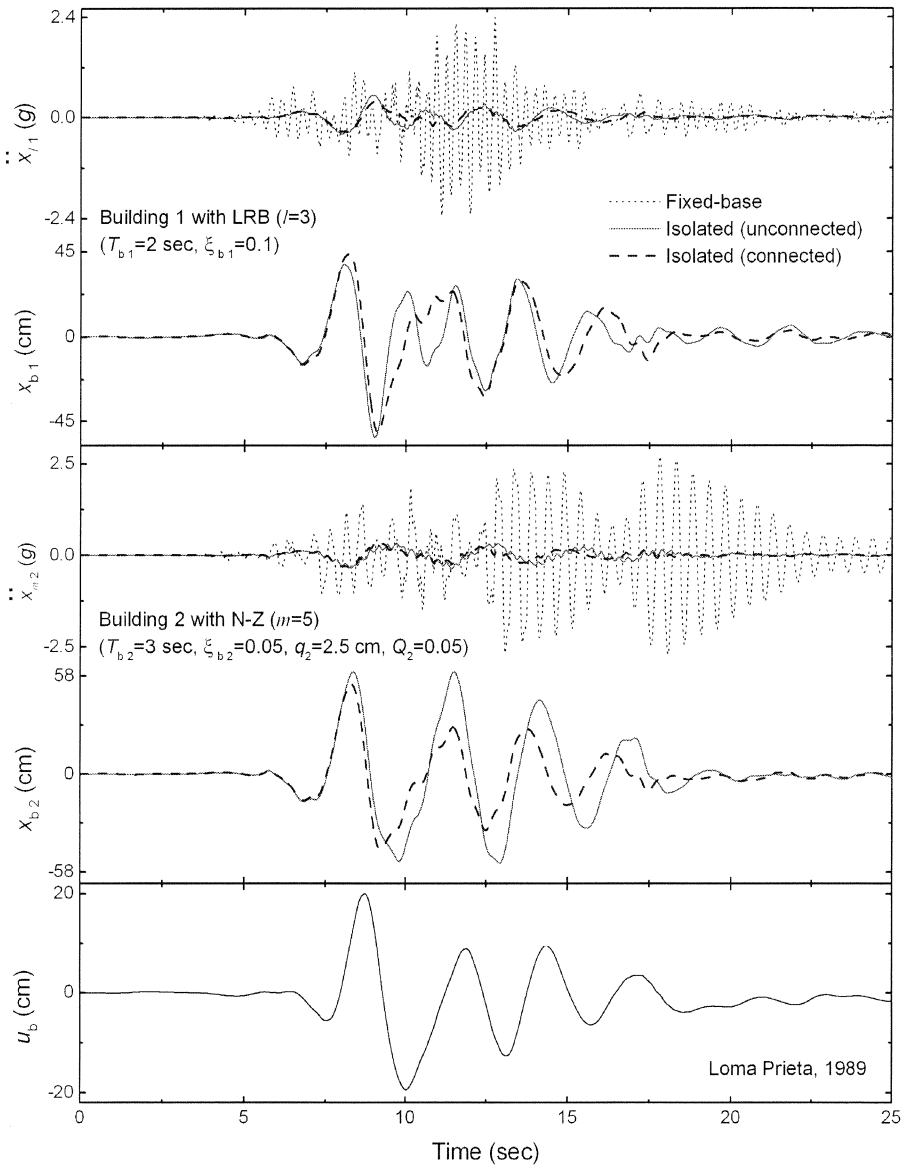

Figure 3.

29

Figure 3. ***Time history for top floor acceleration and bearing displacement for 3 and 5 -storied adjacent base-isolated buildings using LRB and N-Z systems, respectively under Loma Prieta, 1989 earthquake*** ($\eta_d = 2$).

Table 1: Peak response of unconnected and viscous damper connected adjacent base-isolated buildings ($\eta_d = 2$).

Observation quantity		Loma Prieta, 1989		Northridge, 1994		Kobe, 1995	
Isolation system 3-storey Building 1 5-storey Building 2		Bearing displacement (cm)	Top floor acceleration (g)	Bearing displacement (cm)	Top floor acceleration (g)	Bearing displacement (cm)	Top floor acceleration (g)
Unconnected	3-storey LRB	53.38	0.550	34.34	0.362	31.90	0.348
	3-storey N-Z	53.08	0.565	29.92	0.333	34.89	0.393
	5-storey N-Z	60.56	0.380	37.47	0.255	28.95	0.252
	5-storey FPS	63.88	0.436	30.39	0.426	25.30	0.464
Connected	Building 1 LRB	50.68	0.398	37.43	0.306	26.10	0.228
	Building 2 N-Z	52.97	0.366	38.21	0.310	28.92	0.234
	Building 1 LRB	49.02	0.391	34.98	0.301	24.50	0.231
	Building 2 FPS	51.52	0.475	35.98	0.385	26.37	0.368
	Building 1 N-Z	50.03	0.406	34.28	0.307	26.08	0.247
	Building 2 FPS	49.59	0.447	34.54	0.389	25.66	0.360
Non -isolated	3-storey building	-	2.3931	-	1.843	-	2.076
	5-storey building		2.7096		1.965		3.558

dampers to the adjacent Building 1 on different types of isolation systems such as LRB ($T_{b1} = 2\,\text{sec}$ and $\xi_{b1} = 0.1$) and N-Z ($T_{b1} = 2\,\text{sec}$, $\xi_{b1} = 0.05$, $q_1 = 25\,\text{mm}$ and $Q_1 = 0.05$). In few cases, the individual bearing displacement values may increase with the introduction of damper connections, especially for stiffer buildings, however the peak displacement of the combined system (i.e. $x_{b1} + x_{b2}$) reduces considerably as compared to the sum of bearing displacements of these two adjacent base-isolated buildings in unconnected case. This reduction in peak bearing displacement helps in reduced chances of the isolated building system to collide upon the structures on either side of the building such as retaining walls, entrance ramps etc. In no case, however, the top floor acceleration in the isolated building is found to increase than that in case of the corresponding fixed-base Building 1 ($T_{s1} = 0.3\,\text{sec}$

and $\xi_{s1} = 0.02$) and Building 2 ($T_{s2} = 0.5\,\text{sec}$ and $\xi_{s2} = 0.02$).

5.2 Damper Connected Adjacent Base-isolated and Fixed-base Buildings

The time histories of top floor acceleration and bearing displacement for 4-storied base-isolated building supported on LRB ($T_{b1} = 2\,\text{sec}$ and $\xi_{b1} = 0.1$) adjacent to a 6-storied fixed-base building ($T_{s2} = 0.6\,\text{sec}$ and $\xi_{s2} = 0.02$) excited by the Loma Prieta, 1989 earthquake, unconnected and connected using viscous dampers are plotted in Figure 4. The top floor acceleration and base shear, S_{b2} (normalized with weight, W_2) in the fixed-base Building 2 is also shown in Figure 4. The connecting links are provided at all the corresponding adjacent floors of fixed-base and isolated building with $\eta_d = 1.5$. It is observed that there is substantial reduction in the bearing displacement of the base-isolated building and the top floor acceleration in both the base-isolated as well as fixed-base buildings. The bearing displacement of 532.7 mm in the base-isolated Building 1 reduces to 218.5 mm when dampers are placed whereas the top floor acceleration of 0.56g and 2.985g reduces to 0.489g and 2.095g, respectively for the base-isolated Building 1 and fixed-base Building 2. Consequently, the peak values of normalized base shear, S_{b2} in the fixed-base Building 2 has reduced from 0.973 to 0.680. Comparison between Figures 3 and 4 shows that, the effectiveness of viscous damper links to connect the adjacent buildings is more in case of connected base-isolated and fixed-base buildings as compared to the two adjacent connected base-isolated buildings. It also brings forward a very interesting information that an existing fixed-base building can be improved in terms of its seismic performance by constructing a base-isolated building adjacent to it and connecting the two at different floor levels using viscous dampers.

Likewise Table 2 shows some encouraging results of performance of the connected fixed-base and base-isolated buildings using viscous dampers. The peak response of unconnected and connected system between base-isolated and fixed-base buildings for the total normalized external damping $\eta_d = 1.5$ is tabulated. A 4-storied Building 1 isolated using LRB ($T_{b1} = 2\,\text{sec}$ and $\xi_{b1} = 0.1$) is considered adjacent to another 6-storied fixed-base Building 2 ($T_{s2} = 0.6\,\text{sec}$ and $\xi_{s2} = 0.02$). Performance of these two buildings is observed during the cases such as both fixed-base, unconnected and connected at all the floors by viscous dampers with damper damping coefficients equally distributed amongst all the dampers. It is observed that the bearing displacement in Building 1 and top floor accelerations in both the adjacent Buildings 1 and 2 has decreased substantially when viscous damper links are introduced as compared to the top floor acceleration in unconnected cases under Loma Prieta, 1989, Northridge, 1994 and Kobe, 1995 earthquakes. Similar trend of decrease in bearing displacement and top floor accelerations is observed for building on different types of isolation systems, such as FPS and N-Z with similar properties as before, connected to the adjacent fixed-base building using viscous dampers. It can be concluded from these observations that the seismic performance of an existing fixed-base building can be improved by constructing a base-isolated building adjacent to it and connecting these two buildings at different floors using viscous dampers. These damper links also help mitigate the consequences of pounding between the floors of the two buildings adjacent to each other. It can be confirmed that damper connections can be utilized in retrofitting works of the old structures where the separation gap distance is maintained originally from viewpoint of fixed-base building leading to more chances of collision with adjacent structure due to insufficient gap distance than that required for a base-isolated building.

5.3 Optimum Damping of the Viscous Dampers

A parametric study is carried out to observe the effect of externally added damping in the form of viscous damper links at various floor levels of the adjacent base-isolated buildings. The externally added damping is varied while keeping other structural properties of the system constant and superstructure acceleration and bearing displacement is plotted against normalized damper damping, η_d as shown in Figures 5, 6 and 7. In Figure 5, the variation of top floor acceleration and bearing displacement of adjacent base-isolated buildings using LRB and N-Z connected at all floor

levels under Loma Prieta, 1989, Northridge, 1994 and Kobe, 1995 earthquakes is shown, with isolation properties same as before. It can be observed that with the increase in damping of connecting viscous damper the top floor acceleration for isolated Building 1 decreases. On the other hand, in case of the isolated Building 2, the top floor acceleration goes on increasing with increase in external damping.

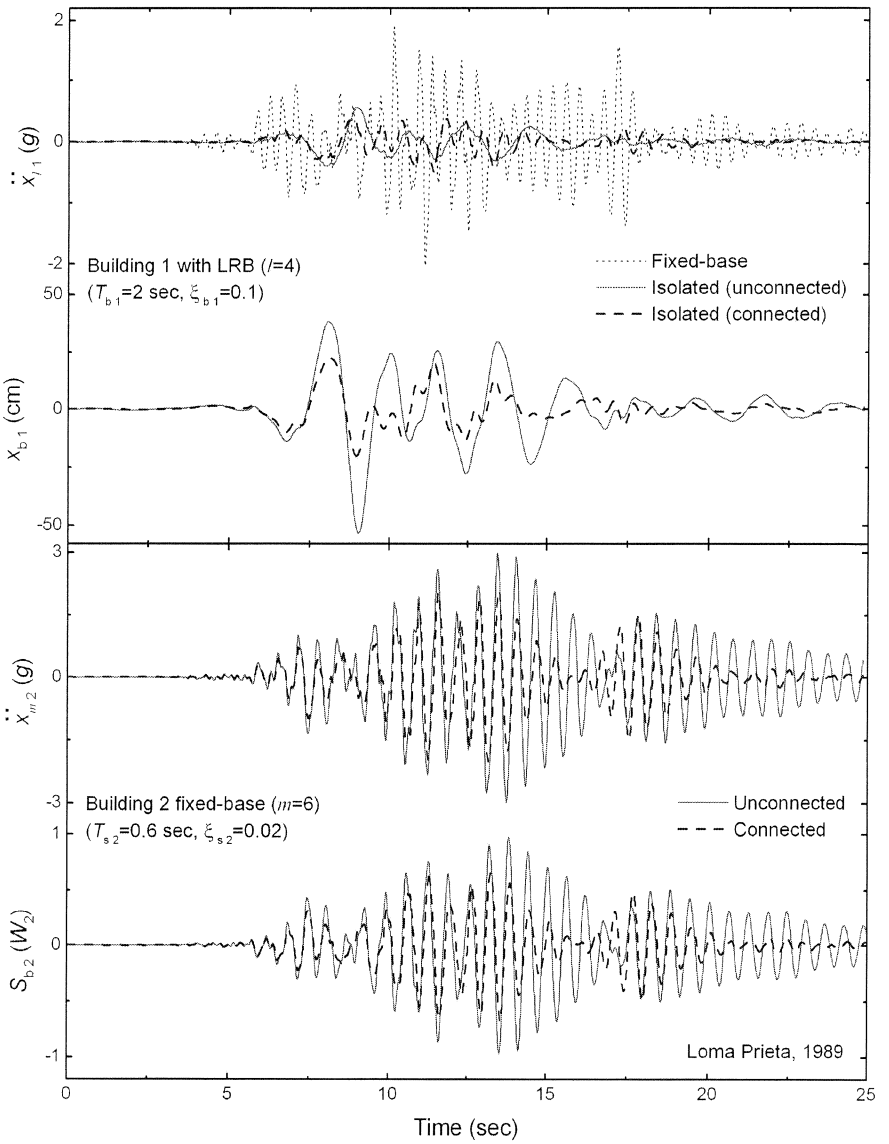

Figure 4.

Figure 4. *Time history for top floor acceleration and bearing displacement of 4-storied base-isolated building using LRB and top floor acceleration and base shear in 6-storied fixed-base adjacent buildings under Loma Prieta, 1989 earthquake ($\eta_d = 1.5$).*

Table 2: Peak response of unconnected and viscous damper connected adjacent base-isolated and fixed-base buildings ($\eta_d = 1.5$).

Observation quantity		Loma Prieta, 1989		Northridge, 1994		Kobe, 1995	
Isolation system 4-storey Building 1 6-storey Building 2		Bearing displacement (cm)	Top floor acceleration (g)	Bearing displacement (cm)	Top floor acceleration (g)	Bearing displacement (cm)	Top floor acceleration (g)
Unconnected	4-storey LRB	53.27	0.560	34.54	0.362	31.34	0.358
	4-storey N-Z	52.97	0.569	30.07	0.339	34.32	0.404
	4-storey FPS	52.05	0.641	31.94	0.482	30.60	0.416
Connected	Building 1 LRB	21.85	0.489	13.76	0.391	13.08	0.416
	Building 2 Fixed	-	2.095	-	1.523	-	1.869
	Building 1 N-Z	20.27	0.477	14.52	0.412	13.43	0.431
	Building 2 Fixed	-	2.101	-	1.528	-	1.871
	Building 1 FPS	19.58	0.623	13.43	0.451	12.53	0.589
	Building 2 Fixed	-	2.120	-	1.590	-	1.849
Non - isolated	4-storey building	-	2.033	-	1.648	-	3.524
	6-storey building		2.985		1.823		2.563

The bearing displacement for both the isolated Buildings 1 and 2 decreases with increase in external damping added with the introduction of damper links initially up to a certain value and with further increase in external damping the bearing displacement in the Building 1 starts increasing while that in the Building 2 showing nearly similar trend. To determine optimum value of external damping for maximum response reduction in a particular damper-linked system, the mean value of peak bearing displacements of the two adjacent base-isolated Buildings 1 and 2 is considered and plotted against the normalized externally added damper values. The minimum value of such mean bearing displacement for the two connected buildings thus obtained from the curve is referred to as the optimum damping for the structural system under investigation. Figure 6 shows the similar plots of top floor acceleration and bearing displacement obtained for two adjacent viscous damper connected base-isolated buildings on LRB and FPS, while Figure 7 that for the two adjacent viscous damper connected base-isolated buildings on N-Z and FPS. Although the trends of results obtained under different earthquakes for different system configuration vary largely, it can be concluded that

for each combination optimum value of externally added damping can be arrived at to obtain the maximum response reduction and the regions where the vulnerable response is obtained can be avoided while designing.

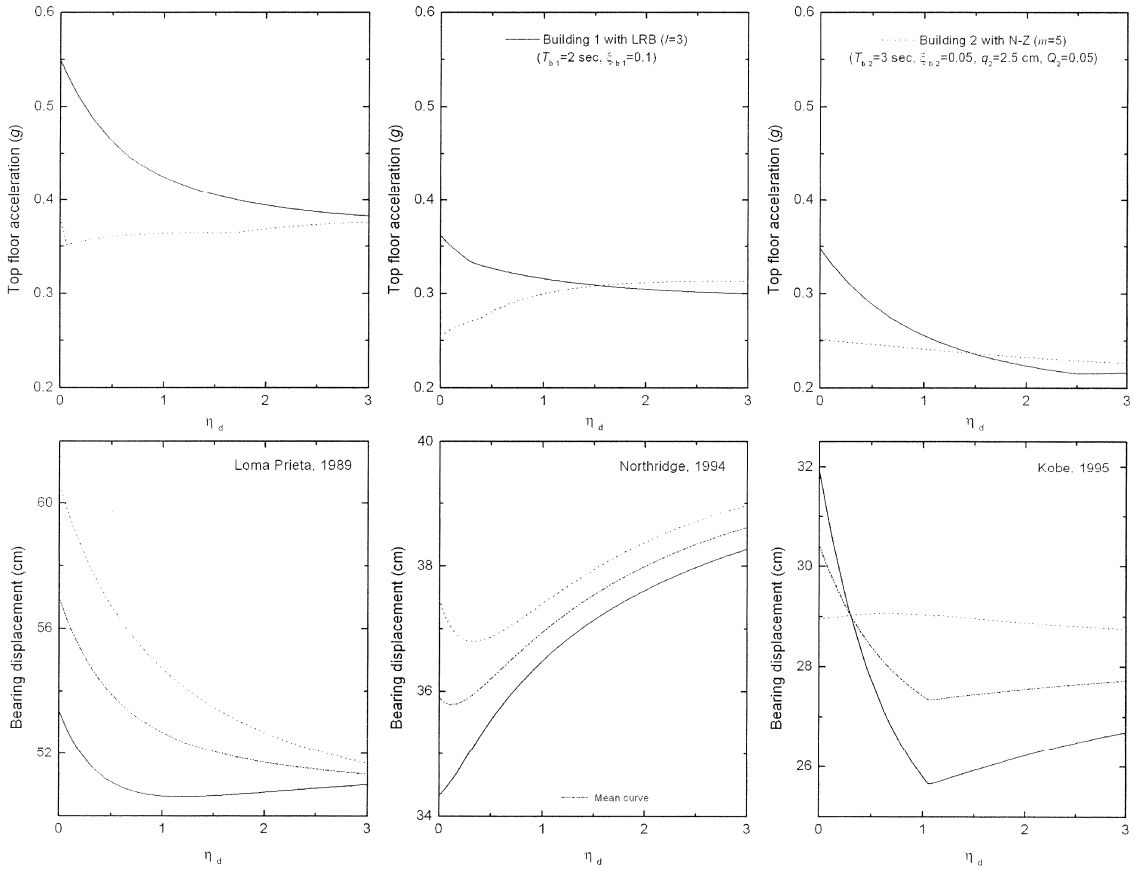

Figure 5.

Figure 5. ***Effect of damping in connecting viscous damper on top floor acceleration and bearing displacement for adjacent base-isolated buildings on LRB and N-Z under different earthquakes.***

5.4 Optimum Placement of Viscous Dampers

It is essential that the use of dampers is made effectively and economically, which necessitates proper selection of the damper damping and its placement. Hence, in order to arrive at efficient distribution pattern of dampers along height of the isolated building to achieve maximum reduction in the response, a parametric study is conducted. The total normalized externally added damping value is maintained constant at $\eta_d = 2$ distributed equally amongst all the viscous dampers used for the connection. The peak response obtained for two adjacent connected base-isolated buildings using different damper distribution patterns is shown in Table 3. It is observed in case of the connected adjacent base-isolated buildings that although response reduction is achieved in all the cases with the introduction of viscous dampers, when a damper is placed at the base-raft for connection, there is maximum response reduction as compared to the other damper distribution patterns with the same overall externally added damping value. This is because the peak differential displacement, u_j across the

dampers occurs at this location, producing higher force, F_d in the damper; therefore, more damping comes into play during the earthquake event. The viscous dampers to be used at this location should be of optimum damping to achieve maximum response reduction. It is to be noted that in the particular system configuration selected here, the placement of dampers showed little effect while for other system configurations it may be crucial criteria to select the optimum placement.

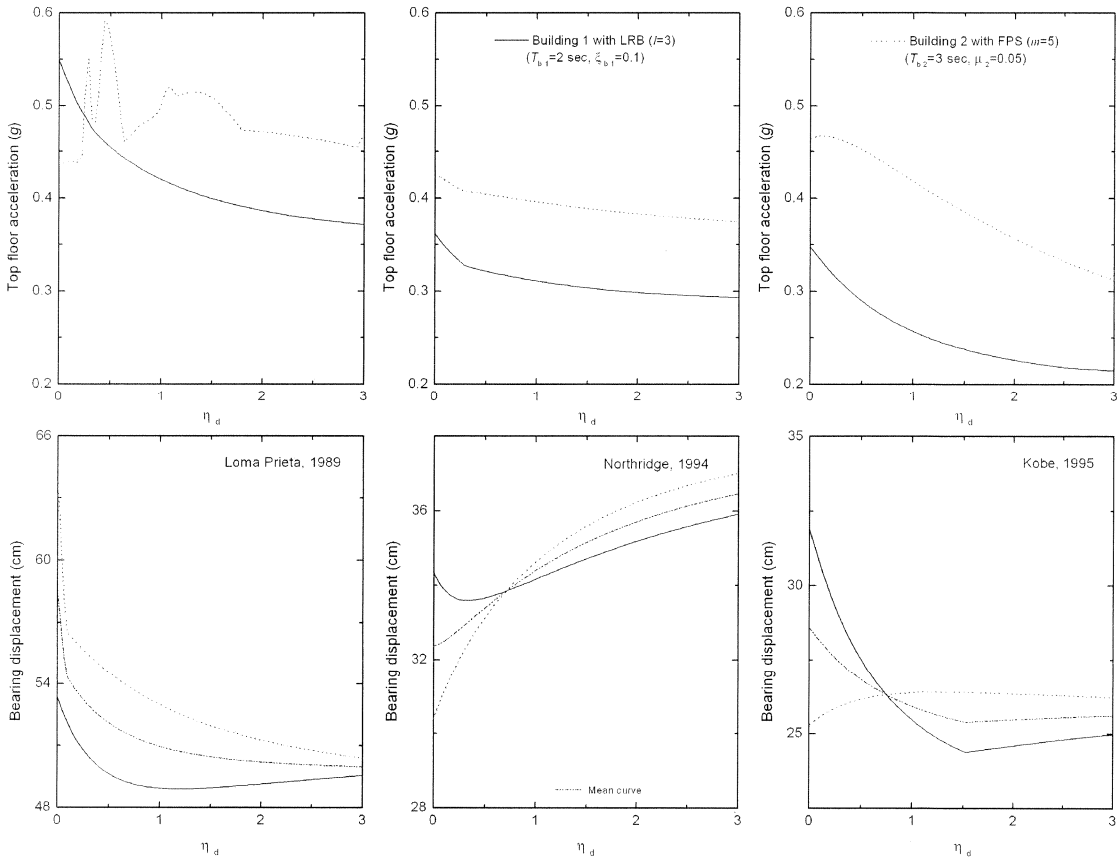

Figure 6.

Figure 6. Effect of damping in connecting viscous damper on top floor acceleration and bearing displacement for adjacent base-isolated buildings on LRB and FPS under different earthquakes.

In case of the connected building system including the base-isolated and fixed-base buildings (Table 4), the maximum response reduction in the fixed-base building is seen when the top floor of base-isolated building is connected using viscous damper to the corresponding floor of adjacent fixed-base building. Therefore, it is advisable to introduce a viscous damper connection between the topmost floor of the base-isolated building and corresponding floor of the fixed-base building to achieve maximum response reduction.

5.5 Effect of Isolation Time Periods

It is quite imperative to study influence of the isolation time period on the seismic response of viscous damper connected base-isolated and fixed-base buildings from viewpoint of arriving at proper selection of the viscous damper properties and its distribution pattern for the adjacent building system under consideration. The variation of top floor acceleration and bearing displacement is plotted against the isolation time period of Building 1, (T_{b1}) while the isolation time period

of Building 2, (T_{b2}) is maintained constant as shown in Figures 8, 9 and 10 for different adjacent base-isolated buildings connected with viscous dampers. The plots are obtained by using normalized values of top floor acceleration and bearing displacement in connected case to that in the unconnected case as follows

$$\Gamma_1 = \frac{(\ddot{x}_{ji})_{connected}}{(\ddot{x}_{ji})_{unconnected}} \qquad (i = 1, 2 \text{ and } j = l, m) \quad (11)$$

$$\Gamma_2 = \frac{(x_{bi})_{connected}}{(x_{bi})_{unconnected}} \qquad (i = 1, 2) \quad (12)$$

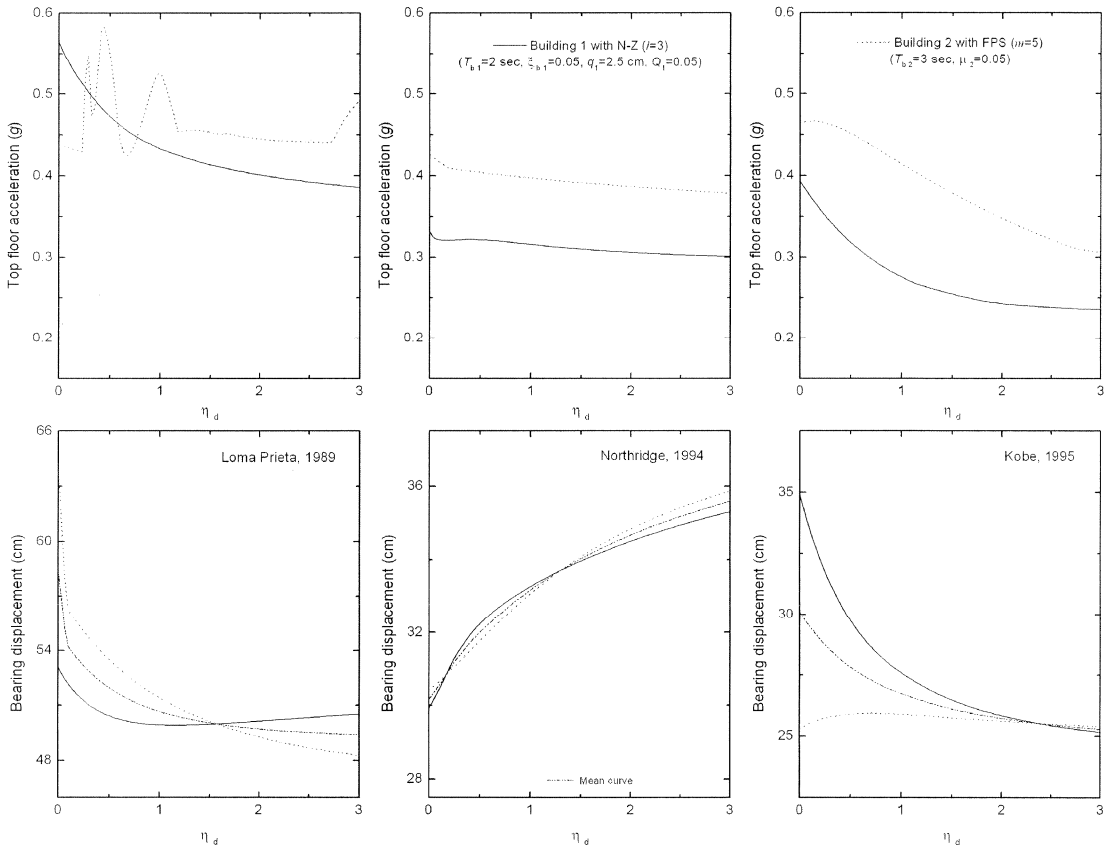

Figure 7.

Figure 7. ***Effect of damping in connecting viscous damper on top floor acceleration and bearing displacement for adjacent base-isolated buildings on N-Z and FPS under different earthquakes.***

In three distinct cases, a 3-storied Building 1 isolated using either of LRB, N-Z and FPS connected using viscous dampers at all the floor levels to an adjacent 5-storied Building 2 isolated using LRB is excited under Loma Prieta, 1989 and Northridge, 1994 earthquakes. The resulting top floor acceleration and bearing displacement for the connected system normalized with that of the unconnected system plotted against the isolation time period of Building 1, (T_{b1}) are as shown in Figure 8. It is observed that the viscous damper links helps in reducing the bearing displacements of the combined system because of additional damping, with marginal increase in the superstructure acceleration.

Table 3: Comparison of peak response of two adjacent connected base-isolated buildings for different damper layouts ($\eta_d = 2$).

Distribution pattern*	Loma Prieta, 1989				Northridge, 1994				Kobe, 1995			
	$\ddot{x}_{l1}$ (g)	$\ddot{x}_{m2}$ (g)	x_{b1} (cm)	x_{b2} (cm)	$\ddot{x}_{l1}$ (g)	$\ddot{x}_{m2}$ (g)	x_{b1} (cm)	x_{b2} (cm)	$\ddot{x}_{l1}$ (g)	$\ddot{x}_{m2}$ (g)	x_{b1} (cm)	x_{b2} (cm)
3-storey building with LRB (T_{b1}=2 sec, ξ_{b1}=0.1) connected to 5-storey building with N-Z (T_{b2}=3 sec, ξ_{b2}=0.05, q_2=2.5 cm, Q_2=0.05)												
All floors connected	0.398	0.366	50.68	52.97	0.306	0.310	37.43	38.21	0.228	0.234	26.10	28.92
Lowermost 3 floors	0.398	0.365	50.65	53.00	0.308	0.308	37.40	38.20	0.227	0.227	26.08	28.91
Base-raft and top floor	0.399	0.362	50.71	52.96	0.304	0.304	37.44	38.18	0.230	0.230	26.11	28.89
Lowermost 2 floors	0.398	0.361	50.61	53.00	0.307	0.302	37.38	38.18	0.225	0.218	26.06	28.89
Base-rafts	0.395	0.356	50.56	53.04	0.303	0.294	37.34	38.16	0.228	0.210	26.03	28.88
Unconnected	0.549	0.380	53.38	60.56	0.362	0.255	34.33	37.47	0.348	0.251	31.90	28.96
3-storey building with LRB (T_{b1}=2 sec, ξ_{b1}=0.1) connected to 5-storey building with FPS (T_{b2}=3 sec, μ_2=0.05)												
All floors connected	0.391	0.475	49.02	51.52	0.301	0.385	34.98	35.98	0.231	0.368	24.50	26.37
Lowermost 3 floors	0.390	0.463	49.00	51.51	0.300	0.384	34.98	36.00	0.227	0.351	24.50	26.39
Base-raft and top floor	0.394	0.476	49.03	51.48	0.302	0.393	35.01	35.97	0.236	0.358	24.48	26.32
Lowermost 2 floors	0.388	0.461	48.93	51.45	0.297	0.387	35.00	36.04	0.232	0.340	24.47	26.37
Base-rafts	0.393	0.457	48.87	51.48	0.302	0.393	34.99	36.07	0.237	0.336	24.43	26.33
Unconnected	0.549	0.436	53.38	63.87	0.362	0.426	34.34	30.39	0.348	0.464	31.90	25.30
3-storey building with N-Z (T_{b1}=2 sec, ξ_{b1}=0.05, q_1=2.5 cm, Q_1=0.05) connected to 5-storey building with FPS (T_{b2}=3 sec, μ_2=0.05)												
All floors connected	0.406	0.447	50.03	49.59	0.307	0.389	34.28	34.54	0.247	0.360	26.08	25.66
Lowermost 3 floors	0.405	0.449	50.01	49.58	0.308	0.387	34.26	34.52	0.247	0.341	26.05	25.67
Base-raft and top floor	0.410	0.453	50.05	49.55	0.308	0.398	34.32	34.52	0.251	0.351	26.09	25.62
Lowermost 2 floors	0.405	0.455	49.96	49.54	0.306	0.387	34.27	34.51	0.251	0.332	26.02	25.65
Base-rafts	0.412	0.455	49.93	49.58	0.309	0.392	34.27	34.51	0.253	0.318	25.99	25.62
Unconnected	0.565	0.436	53.08	63.87	0.333	0.426	29.93	30.39	0.393	0.464	34.89	25.30

* with reference to Building 1.

Table 4: Comparison of peak response of adjacent connected base-isolated and fixed-base buildings for different damper layouts ($\eta_d = 1.5$).

Distribution pattern*	Loma Prieta, 1989			Northridge, 1994			Kobe, 1995		
	$\ddot{x}_{l1}$ (g)	$\ddot{x}_{m2}$ (g)	x_{b1} (cm)	$\ddot{x}_{l1}$ (g)	$\ddot{x}_{m2}$ (g)	x_{b1} (cm)	$\ddot{x}_{l1}$ (g)	$\ddot{x}_{m2}$ (g)	x_{b1} (cm)
4-storey building with LRB (T_{b1}=2 sec, ξ_{b1}=0.1) connected to 6-storey fixed-base building (T_{s2}=0.6 sec, ξ_{s2}=0.02)									
All floors connected	0.489	2.095	21.85	0.391	1.523	13.76	0.416	1.869	13.08
Lowermost 3 floors	0.494	2.379	21.94	0.386	1.629	13.61	0.428	2.010	12.78
Lowermost and top floor	0.452	2.059	21.91	0.372	1.479	13.81	0.429	1.866	13.10
Lowermost 2 floors	0.467	2.654	22.03	0.364	1.715	13.61	0.443	2.179	12.60
Lowermost floor	0.419	2.861	22.11	0.336	1.762	13.81	0.444	2.361	12.57
Topmost floor	0.493	1.697	21.78	0.414	1.255	14.89	0.456	1.636	14.77
Unconnected	0.559	2.987	53.02	0.362	1.823	34.54	0.358	2.563	31.34
4-storey building with N-Z (T_{b1}=2 sec, ξ_{b1}=0.05, q_1=2.5 cm, Q_1=0.05) connected to 6-storey fixed-base building (T_{s2}=0.6 sec, ξ_{s2}=0.02)									
All floors connected	0.477	2.100	20.27	0.412	1.528	14.52	0.431	1.871	13.43
Lowermost 3 floors	0.482	2.384	20.24	0.408	1.633	14.28	0.434	2.011	13.20
Lowermost and top floor	0.443	2.066	20.34	0.392	1.483	14.56	0.440	1.868	13.46
Lowermost 2 floors	0.461	2.656	20.31	0.389	1.719	14.16	0.448	2.178	13.11
Lowermost floor	0.418	2.860	20.47	0.365	1.765	14.25	0.457	2.357	13.18
Topmost floor	0.507	1.702	20.93	0.433	1.257	15.81	0.479	1.630	15.08
Unconnected	0.568	2.987	52.74	0.339	1.823	30.07	0.404	2.563	34.32
4-storey building with FPS (T_{b1}=2 sec, μ_1=0.05) connected to 6-storey fixed-base building (T_{s2}=0.6 sec, ξ_{s2}=0.02)									
All floors connected	0.623	2.124	19.57	0.451	1.590	13.43	0.589	1.849	12.53
Lowermost 3 floors	0.667	2.401	19.01	0.437	1.675	13.07	0.592	1.995	12.33
Lowermost and top floor	0.565	2.101	19.56	0.433	1.558	13.47	0.506	1.835	12.56
Lowermost 2 floors	0.664	2.686	18.73	0.458	1.749	12.83	0.515	2.157	12.36
Lowermost floor	0.626	2.890	18.74	0.480	1.782	12.87	0.562	2.370	12.55
Topmost floor	0.631	1.746	20.40	0.483	1.346	14.97	0.619	1.669	14.87
Unconnected	0.640	2.987	51.82	0.482	1.823	31.94	0.416	2.563	30.60

* with reference to fixed-base building.

In almost all the cases, increase in the superstructure acceleration due to damper connections ranges about 25 percent than that during the unconnected case whereas reduction achieved in the bearing displacement due to damper connections is as high as 50 percent. Similar observations can be made from Figures 9 and 10, plotted for different combinations of isolated buildings mounted on various isolation systems. It can also be seen from these figures that the response reduction obtained after introduction of viscous dampers is more when the isolation systems used beneath the two adjacent buildings are having large difference in the isolation time periods and when the isolation systems are of dissimilar type. This is attributed towards the fact that for different kind of isolation systems and time periods, the vibration phase difference results in more differential displacement, u_j at different floor levels across the viscous dampers. The effectiveness of viscous damper links is found to be more at higher values of isolation time periods. It is also observed that when the ratio of time periods is unity the advantages obtained in using the dampers are insignificant. Thus, it is advisable to use dampers as connection links to connect the adjoining floors of the structures when the time periods are well separated.

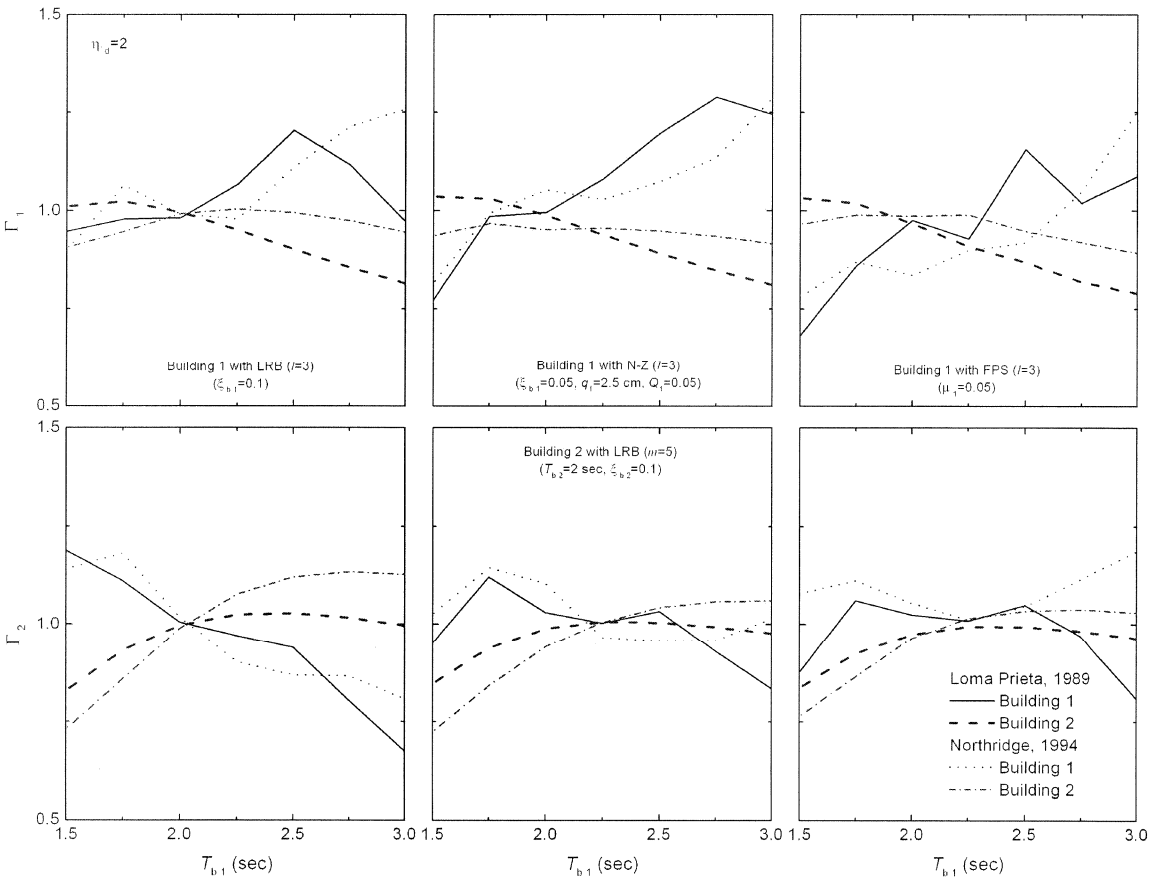

Figure 8.

Figure 8. Response ratio against the isolation time period of the base-isolated buildings on LRB, N-Z and FPS connected to the adjacent building on LRB by viscous dampers under different earthquakes.

5.6 Effect of Superstructure Flexibility

In order to study the effects of flexibility of the superstructure of these adjacent connected buildings, the peak values of top floor acceleration and bearing displacement are obtained for a 4-storied base-isolated building using LRB connected at all the corresponding floors of 6-storied fixed-base building under different earthquakes with $\eta_d = 1.5$ as shown in Figure 11. It is observed from these plots that the reduction in superstructure acceleration is more when the superstructure is flexible (i.e. at the higher time period of the superstructure). Moreover, the bearing displacement shows no variation with the changes in fundamental time period of the superstructure. This implies that the effectiveness of dampers in connecting the isolated buildings increases with the increased superstructure flexibility.

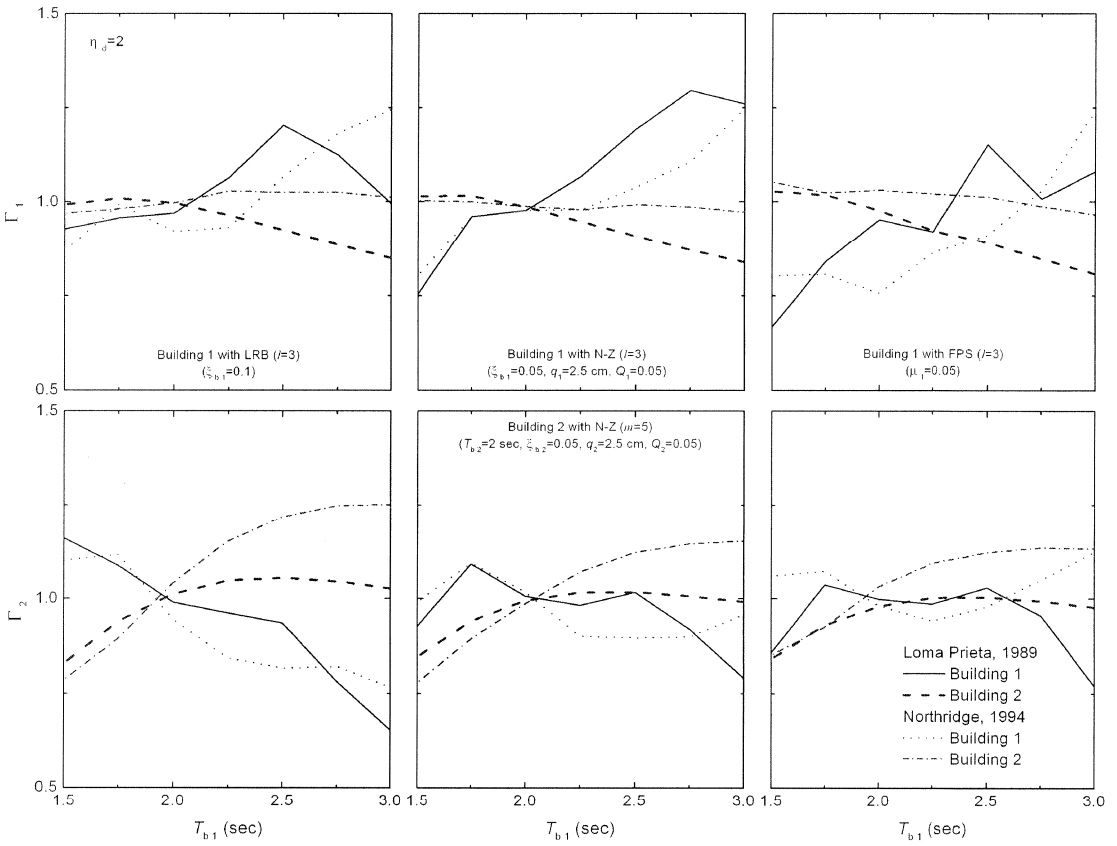

Figure 9.

Figure 9. Response ratio against the isolation time period of the base-isolated buildings on LRB, N-Z and FPS connected to the adjacent building on N-Z by viscous dampers under different earthquakes.

6.0 CONCLUSIONS

Seismic response of dissimilar adjacent buildings connected with viscous dampers is investigated, when both or one of the buildings is base-isolated. Parametric study is conducted on adjacent shear type of base-isolated structure to observe the influence of different parameters of adjacent structures and the viscous damper links. Optimal parameters such as damping and its location are obtained for viscous dampers used as connecting links to achieve maximum response reduction during earthquake excitations. From the trend of

the results of present study, following conclusions can be drawn.

1. Significant reduction in the peak bearing displacement is achieved by introducing viscous damper connections at the floor levels of adjacent base-isolated buildings, helpful in avoiding the consequences of pounding. Superstructure acceleration in the stiffer base-isolated building may increase marginally due to the introduction of dampers as connectors; nevertheless, it remains much lower than that in the corresponding fixed-base system;
2. The effectiveness of viscous dampers as connecting links is found to be significantly more in case of connected base-isolated and fixed-base buildings as compared to the two adjacent base-isolated buildings with damper connection;
3. Damper connections are more useful in dissimilar kind of isolation systems for the two adjacent base-isolated buildings. For similar type of isolation systems, the advantages of damper usage are insignificant;
4. The effectiveness of viscous damper links increases with increase in superstructure flexibility of the adjacent connected buildings;
5. An optimum value of externally added damping criterion can be arrived at to obtain the maximum response reduction in the two connected buildings;

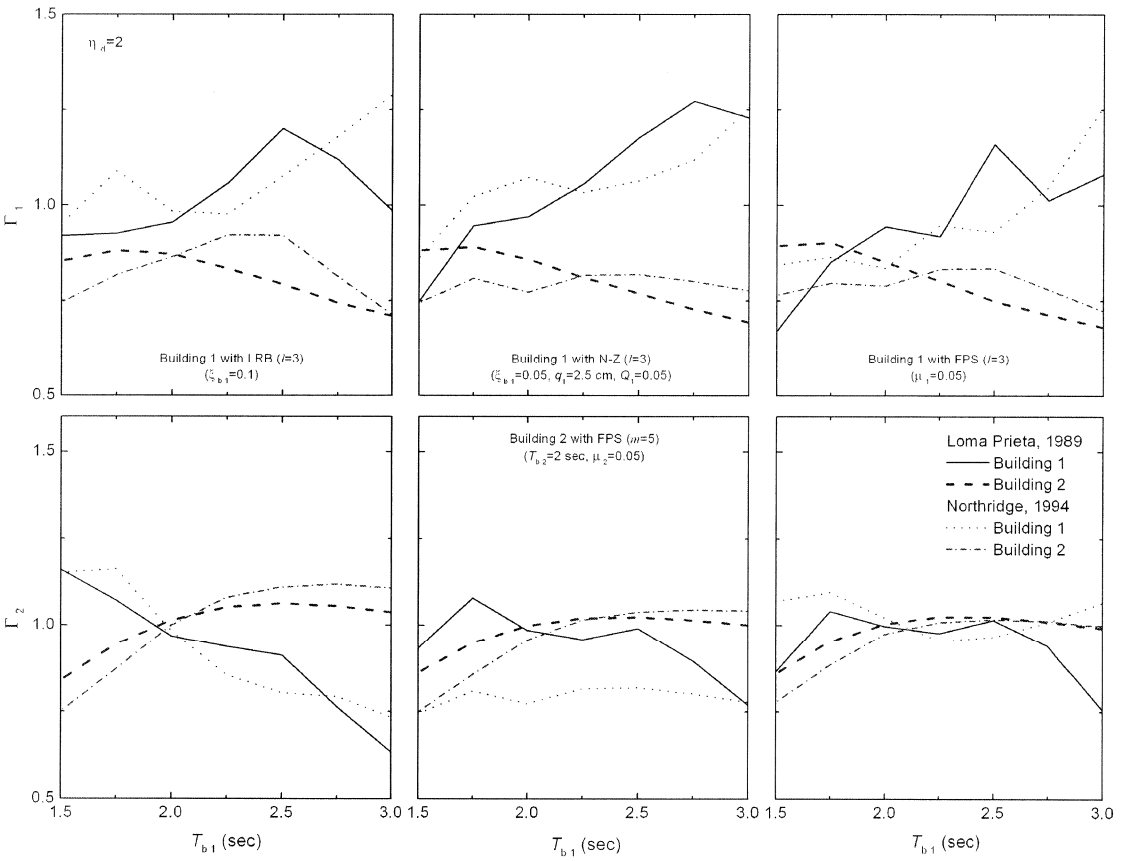

Figure 10.

Figure 10. Response ratio against the isolation time period of the base-isolated buildings on LRB, N-Z and FPS connected to the adjacent building on FPS by viscous dampers under different earthquakes.

6. Maximum response reduction is observed when the base-rafts of adjoining base-isolated buildings are connected using viscous dampers. Moreover, connecting the topmost floor of base-isolated building to the adjoining floor of fixed-base building using viscous dampers results in maximum response reduction.

REFERENCES

1. Kelly, J.M. "Aseismic base isolation: review and bibliography", *Soil Dynamics and Earthquake Engineering*, 1986; **5**(3): 202-216.
2. Buckle, I.G. and Mayes R.L. "Seismic isolation: history, application and performance- a world view", *Earthquake Spectra*, 1990; **6**(2): 161-201.
3. Jangid, R.S. and Datta T.K. "Seismic behavior of base-isolated buildings: a state-of-the-art review", *Structures and Buildings*, 1995; **110**(2): 186-203.
4. International Conference of Building Officials. "Earthquake regulations for seismic isolated structures", *Uniform Building Code*, 1997; Whittier, CA.

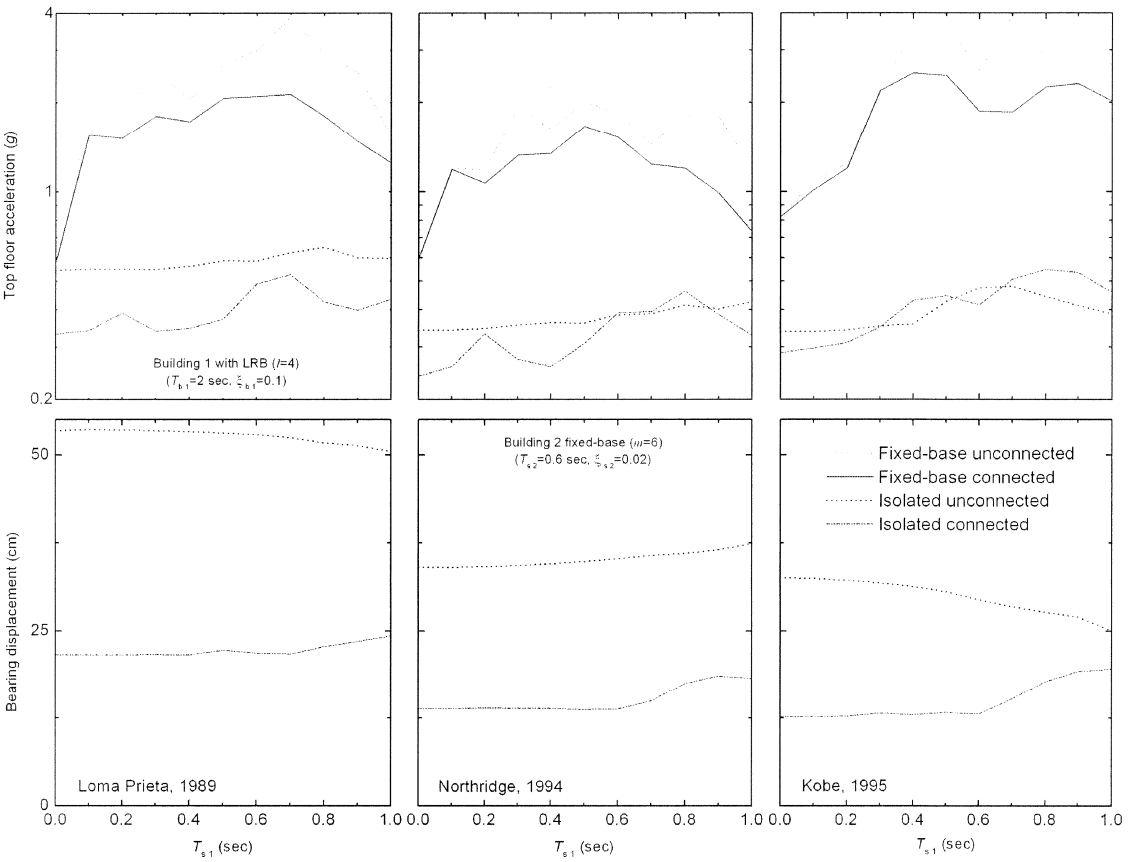

Figure 11.

Figure 11. Effect of superstructure flexibility on response of connected and unconnected adjacent isolated 4-storied building on LRB and fixed-base 6-storied building connected by viscous dampers under different earthquakes ($\eta_d = 1.5$).

5. Housner, G.W., Bergman L.A., Caughey T.K., Chassiakos A.G., Claus R.O., Masri S.F., Skelton R.E., Soong T.T., Spencer Jr. B.F. and Yao J.T.P. "Structural control: past, present and future", *Journal of Engineering Mechanics* (ASCE), 1997; **123**(9): 897-971.
6. Soong, T.T. and Spencer Jr. B.F. "Supplemental energy dissipation: state-of-the-art and state-of-the-practice", *Engineering Structures*, 2002; **24**(3): 243-259.
7. Westermo, B.D. "The dynamics of interstructural connection to prevent pounding", *Earthquake Engineering and Structural Dynamics*, 1989; **18**(5): 687-699.
8. Luco, J.E. and De Barros F.C.P. "Optimal damping between two adjacent elastic structures", *Earthquake Engineering and Structural Dynamics*, 1998; **27**(7): 649-659.
9. Xu, Y.L. and Zhang W.S. "Closed-form solution for seismic response of adjacent buildings with linear quadratic Gaussian controllers", *Earthquake Engineering Structural Dynamics*, 2002; **31**(2): 235-259.
10. Xu, Y.L., He Q. and Ko J.M. "Dynamic response of damper-connected adjacent buildings under earthquake excitation", *Engineering Structures*, 1999; **21**(2): 135-148.
11. Xu, Y.L., Zhan S., Ko J.M. and Zhang W.S. "Experimental investigation of adjacent buildings connected by fluid damper", *Earthquake Engineering and Structural Dynamics*, 1999; **28**(6): 609-631.
12. Ni, Y.Q., Ko J.M. and Ying Z.G. "Random seismic response analysis of adjacent buildings coupled with non-linear hysteretic dampers", *Journal of Sound and Vibration*, 2001; **246**(3): 403-417.
3. Zhang, W.S. and Xu Y.L. "Dynamic characteristics and seismic response of adjacent buildings linked by discrete dampers", *Earthquake Engineering and Structural Dynamics*, 1999; **28**(10): 1163-1185.
14. Zhang, W.S. and Xu Y.L. "Vibration analysis of two buildings linked by Maxwell model-defined fluid dampers", *Journal of Sound and Vibration*, 2000; **233**(5): 775-796.
15. Constantinou, M.C., Symans M.D., Tsopelas P., and Taylor D.P. "Fluid viscous dampers in applications of seismic energy dissipation and seismic isolation", *Proceedings of seminar on seismic isolation, passive energy dissipation and active control*, Report No. ATC-17-1, Applied Technology Council, San Francisco, CA, 1993; 2: 581-592.
16. Kelly, J.M. "Earthquake resistant design with rubber", *Springer Publishers*, 1997; New York, USA.
17. Robinson, W.H. "Lead-rubber hysteretic bearings suitable for protecting structures during earthquakes", *Earthquake Engineering and Structural Dynamics*, 1982; **10**(4): 593-604.
18. Wen, Y.K. "Method for random vibration of hysteretic systems", *Journal of the Engineering Mechanics Division* (ASCE), 1976; **102**(2): 249-263.
19. Zayas, V.A., Low S.S. and Mahin S.A. "A simple pendulum technique for achieving seismic isolation", *Earthquake Spectra*, 1990; **6**(2): 317-333.